



# Microstructure and Mechanical Properties of Magnesium-Aluminium (Mg-Al) Alloys with High Aluminium Content (Al = 10, 15, 20 wt. %)

S Jayalakshmi<sup>a</sup>, R Arvind Singh<sup>a\*</sup>, Sanjay Mohan<sup>b</sup>, S Sankaranarayanan<sup>c</sup>, Vasco Machemba Gomano<sup>a</sup>, Xizhang Chen<sup>a</sup> & Manoj Gupta<sup>c</sup>

<sup>a</sup>College of Mechanical and Electrical Engineering, Wenzhou University, Wenzhou 325 035, China

<sup>b</sup>School of Mechanical Engineering, Shri Mata Vaishno Devi University, Kakryal, Katra, Jammu and Kashmir 182 320, India

<sup>c</sup>Department of Mechanical Engineering, 9 Engineering Drive 1, National University of Singapore (NUS), Singapore 117 576

Received 27 January 2021; accepted 17 February 2021

Magnesium-Aluminium (Mg-Al) alloys containing zinc or manganese are preferred choice in automobile and aerospace sectors. Aluminium, the major strengthening element in Mg-alloys is always added below its solid solubility limit of 12.5 wt.%. In the current study, Mg-Al binary systems with Al-content just below and above the solubility limit (Al = 10, 15 and 20 wt.%) were developed and examined for their microstructural and mechanical behaviour. Microstructural studies showed the importance of Al-content in determining: (i) grain size reduction and (ii) distribution and amount of inter metallic phase. Mechanical property evaluation showed that the hardness increase was linearly dependent on Al-content, with Mg-20Al showing > 250% increase in hardness than commercial AZ91alloy. Mg-10Al showed 215% and 130% increase in yield and ultimate strengths respectively, and exhibited the best properties in terms of work of fracture, which is representative of the alloy's toughness.

**Keywords:** Magnesium alloys, Aluminium, Microstructure, Intermetallic phase, Mechanical behaviour

## 1 Introduction

Magnesium-based alloys (Mg-alloys) are promising materials for automotive industries<sup>1</sup> owing to their low density (1.74 g/cm<sup>3</sup>). Magnesium is generally alloyed with aluminium, manganese, copper, rare earth metals, silicon, and zirconium *etc.*<sup>2</sup>. The widely used commercial Mg-alloys contain aluminium, as in: (i) AZ series (Mg-Al-Zn system, *e.g.* AZ91, AZ31 alloys), (ii) AM series (Mg-Al-Mn system, *e.g.* AM50, AM60 alloys), (iii) AS series (Mg-Al-Si system, *e.g.* AS21, AS41 alloys) and (iv) AE series (Mg-Al-Rare Earth system, with AE42 alloy as an example)<sup>2,3</sup>. These alloys are preferred due to their excellent castability, secondary processing ability and precipitation hardening capability<sup>4</sup>. Incorporating aluminium to Mg, in combination with other minor elements render high specific strength when compared to several Al-based alloys and provides better corrosion resistance<sup>4,5</sup>. However, the application of Mg-alloys as structural load-bearing members are still limited due to their relatively poor strength as required in specific applications, such as in aerospace and defense sectors. In order to widen the application potential of magnesium alloys, their mechanical properties need to

be enhanced, which can be achieved by the selection of proper amount of alloy constituents or by making metal matrix composites<sup>4</sup>.

Among the various alloying elements used, aluminium is reported to provide the best properties as it acts as a solid solution strengthener, as well as precipitation hardener<sup>1,2,5</sup>. Also, due to its relatively low density (next only to Mg), its addition in effect does not increase the overall weight of alloys significantly. From Mg-Al binary phase diagram, Al-solubility limit in  $\alpha$ -Mg at 710 K is 12.5 weight pct.<sup>6</sup>. The currently used Mg-Al based commercial alloys contain a maximum of 9 wt. % Al, well below the solubility limit. An earlier study reported that Mg-Al binary alloys containing Al exceeding the solubility limit showed significant increase in tensile strength properties<sup>7</sup>.

In the current work, Mg-Al binary alloys containing Al = 10, 15 and 20 weight pct. were developed, considering that aluminium is relatively a cost-effective element which can be utilized for enhancing strength characteristics of magnesium. Mg-Al alloys were fabricated by disintegrated melt deposition (DMD) process, and were then hot-extruded. The fabricated materials were investigated for microstructure and mechanical behaviour. Correlation of microstructural

\*Corresponding author (E-mail: arvindsingh.r@gmail.com)

with mechanical behaviour due to increasing Al-composition is presented.

## 2 Experimental Details

### 2.1 Materials and processing

Mg-turnings (purity: 99.9 pct.) and Al-powder were used as base element and alloying element respectively. Using *DMD* process, three Mg-binary alloy composition with 10, 15 and 20 Al (in weight pct.), namely Mg-10Al, Mg-15Al and Mg-20Al alloys were produced. Figure 1 shows schematic of process set-up<sup>4</sup>. The powders were placed in a layered manner into the crucible containing magnesium turnings, which was then heated to 1023 K with inert Ar-gas (flowing at 2.5 L/min) atmosphere in a resistance furnace, and stirred at 450 rpm for melt homogenization. The molten slurry was made to exit by bottom pouring with two Ar-gas stream disintegrating the melt, which was deposited onto a steel mould. The solidified alloy of diameter 40 millimeter was subsequently machined to 36 millimeter. The billets (held at 673 K, 1 hour) was hot extruded at 623 K (extrusion ratio ~20.25:1) to produce 8 millimeter diameter rods, using which microstructural analysis and mechanical tests were carried out.

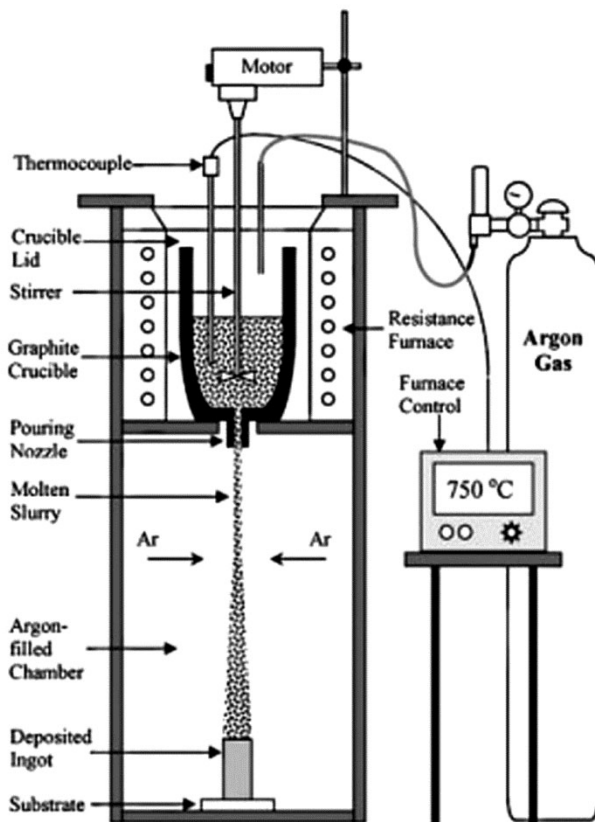


Fig. 1 — Disintegrated melt deposition process set-up

### 2.2 Testing and Analysis

#### 2.2.1 X-ray diffraction (XRD)

Polished samples with heights 5 to 8 mm were exposed to copper-K $\alpha$  x-rays ( $\lambda = 1.54056 \text{ \AA}$ ) with scan speed: 2 degree/min, and scan range: 20 to 80 degrees. From the diffraction patterns, crystalline peaks were identified for the respective phases by matching them with standard Mg-peaks, Al-peaks and associated peaks of intermetallic compounds.

#### 2.2.2 Microstructural Analysis

Structural analysis on Mg-10Al, Mg-15Al and Mg-20Al alloys was conducted to examine the morphology of grains and second phase dispersion. After fine polishing, the grain size was observed after etching using an etchant of composition 10 millilitre acetic acid, 95 millilitre ethyl alcohol and 5g picric acid, for about 15 seconds by swabbing method. Grain size was observed in a metallurgical microscope, whereas the distribution of intermetallic phase was studied in a Hitachi field emission scanning electron microscope (*FESEM-S4300*).

#### 2.2.3 Microhardness

Microhardness values were measured on extruded alloys using Vickers indenter (Shimadzu HMV automatic digital microhardness tester, *ASTM* standard E384), conducted at applied load of 245 mN for a duration of 15 seconds. Ten to fifteen readings were obtained on three samples for each alloy composition.

#### 2.3.4 Compression properties

Compressive loading behaviour was evaluated in an automated servo-hydraulic mechanical test machine (Model-*MTS* 810) at a crosshead speed of 0.040 mm/s, on samples with diameter: 8 millimeter and height/diameter ~1. Five tests were performed for each composition, and average values are reported.

#### 2.3.5 Fractography

Fracture surfaces of compression-tested samples were analysed in *FESEM* to identify failure modes.

## 3 Results and Discussion

### 3.1 XRD

Figure 2 shows *XRD* patterns wherein from the crystalline peak intensity analysis, it was identified that in addition to pure Mg peaks ( $\alpha$ -Mg),  $\beta$ -Mg<sub>17</sub>Al<sub>12</sub> secondary phase (the eutectic phase) formed in all the alloys. The obtained peaks given in

Table 1 shows that number of peaks of  $Mg_{17}Al_{12}$  phase increased corresponding to the increase in the Al-content.

### 3.2 Microstructural characterization

Microstructural features of the developed alloys are shown in Fig. 3(a-f), and the details of the observations are summarized in Table 2. From optical micrographs Fig. 3(a-c) and Table 2, it could be observed that the Mg-grain size reduced with as Al-content is increased.

The microstructures of the developed alloys show defect free structure and near-equiaxed grains, and the presence of intermetallic phase (white regions) throughout the  $\alpha$ -Mg matrix. The fine grain size is due to: (i) hot extrusion process which causes dynamic recrystallization of the  $\alpha$ -Mg, (ii)  $Mg_{17}Al_{12}$  phase which serves as active sites for grain nucleation upon hot extrusion and (iii) the presence of the hard  $Mg_{17}Al_{12}$  phase which acts as obstacles for grain growth. In Mg-10Al (Fig. 3 (d)),  $Mg_{17}Al_{12}$  intermetallic is distributed randomly along grain boundaries. The hard and brittle  $Mg_{17}Al_{12}$  intermetallic is known to form a network structure in Mg-Al alloys<sup>8</sup>. The absence of networked structure in Mg-10Al indicates that the hot extrusion process has effectively broken the network structure and has caused a more random distribution. The amount

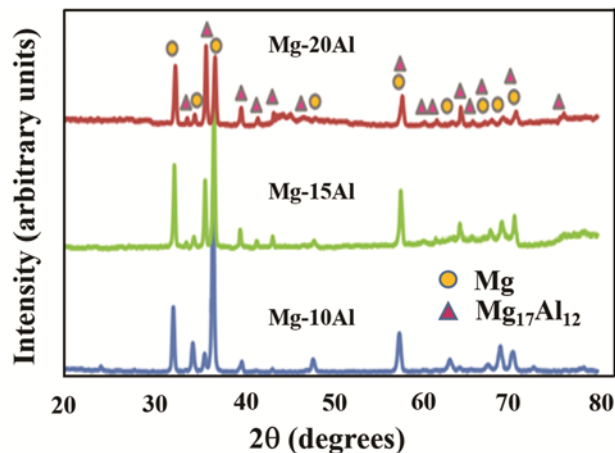


Fig. 2 — X-ray diffraction patterns of Mg-Al binary system (Al = 10, 15 and 20 wt.%).

Table 1 — X-ray diffraction peaks of Mg-Al binary alloys (Al = 10, 15 and 20 wt. %).

Alloy	Mg peaks	$Mg_{17}Al_{12}$ peaks
Mg-10Al	10	7
Mg-15Al	9	11
Mg-20Al	9	14

(area fraction) of the  $Mg_{17}Al_{12}$  intermetallic phase increased significantly with the Al-content<sup>7,9</sup> with a tendency to form grain boundary network structure, as observed in Fig. 3(e). In the Mg-20Al alloy, the  $Mg_{17}Al_{12}$  intermetallic phase content was >70% which segregated and formed a clustered structure (Fig. 3(f)). Due to this reason, the grain size was not measurable, though it is expected to be of fine grain size, as reported by Nguyen *et al.*<sup>7</sup>. The high segregation of  $Mg_{17}Al_{12}$  intermetallic phase along the grain boundaries when Al-content exceeds the solubility limit of 12% was earlier reported by Dargusch *et al.*<sup>10</sup>.

### 3.3 Mechanical behaviour

#### 3.3.1 Microhardness

From the measured microhardness values (Table 3), it seen that hardness values increase significantly with increment in Al wt.%, such that for Mg-20Al, the microhardness value was almost twice as that of

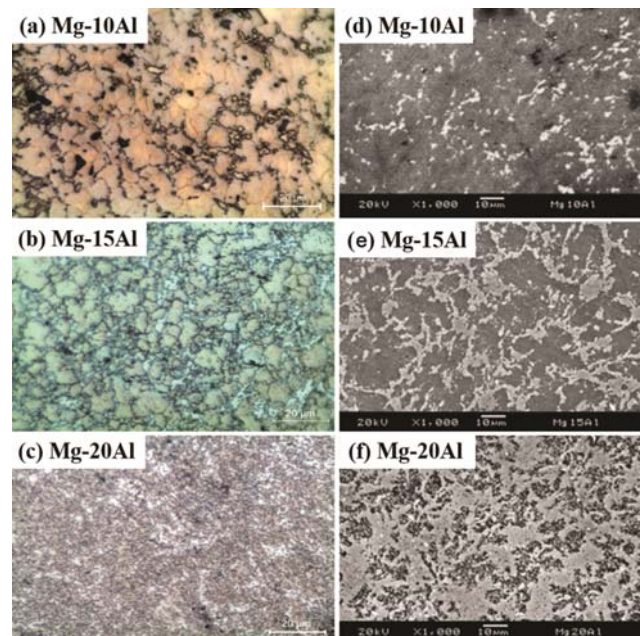


Fig. 3 — Optical microscopic images: (a) Mg-10Al, (b) Mg-15Al and (c) Mg-20Al, showing grain size reduction with increase in Al-content. SEM images that show  $Mg_{17}Al_{12}$  intermetallic distribution (white regions) in: (d) Mg-10Al, (e) Mg-15Al and (f) Mg-20Al, which reveal increase in intermetallic phase formation as Al-content increased.

Table 2 — Grain size and amount of  $Mg_{17}Al_{12}$  intermetallic phase in Mg-Al binary alloys (Al = 10, 15 and 20 wt.%).

Alloy	Grain size ( $\mu m$ )	Amount of $Mg_{17}Al_{12}$ phase (%)
Mg-10Al	$7.50 \pm 1.96$	12
Mg-15Al	$5.47 \pm 1.60$	36
Mg-20Al	-	74

Mg-10Al. Such an increment occurs due to high content of Mg<sub>17</sub>Al<sub>12</sub> intermetallic phase which increases with increase in Al-content. The Mg<sub>17</sub>Al<sub>12</sub> intermetallic phase is inherently hard<sup>2</sup> with a hardness of 280 Hv. Hence, the overall increase in the microhardness values of the developed alloys is due to: (i) presence of high content of hard intermetallic phase, (ii) fine grain size that restricts Mg-deformation during the indentation process<sup>4,11,12</sup> and (iii) the hard Mg<sub>17</sub>Al<sub>12</sub> phase that act as obstacles for dislocation motion<sup>2,3,8,11</sup>. For comparison, the hardness values of pure Mg, Mg-9Al and AZ91 commercial alloy have been listed in Table 3. On comparing with pure Mg, there is a noteworthy enhancement in hardness (*e.g.* Mg-20Al alloy shows 4.6 times increase, *i.e.* more than 300% enhancement). Similarly, increasing the aluminium content by just 1%, *i.e.* Mg-9Al<sup>13</sup> to Mg-10Al increased the hardness value by 15%. The microhardness value of all the developed alloys show much higher values than the commercial AZ91 alloy<sup>13</sup> as mentioned in Table 3.

**3.3.2 Compressive properties**

Table 4 gives the results from compression tests. Increasing addition of aluminium influenced compressive yield strength (CYS) as well as ultimate compressive strength (UCS). Results revealed that compressive yield strength of alloys increased with increase in Al composition, such that from Mg-10Al to Mg-15Al, a 50% increase in compressive yield strength value was observed. The hard Mg<sub>17</sub>Al<sub>12</sub> intermetallic

phase present in the alloys impedes dislocation motion and contributes towards their strength. In Mg-15Al, owing to increased presence of intermetallic (Table 3), it has higher compressive yield strength value than Mg-10Al. Further, ultimate compression strength for Mg-10Al was 545 MPa, and that for Mg-15Al was 458 MPa. This lowering of ultimate strength is because of increased presence of Mg<sub>17</sub>Al<sub>12</sub> phase which is brittle in nature. The Mg-20% Al alloy did not show any prominent yield point indicating that 20% Al addition has resulted in the alloy becoming very brittle. This is attributed to the very high content of Mg<sub>17</sub>Al<sub>12</sub> intermetallic phase in Mg-20Al alloy (Table 3) that results in very less plastic deformation (Table 4), and hence undergoes brittle fracture. For comparison, properties of pure Mg have also been listed in Table 4, wherein the developed alloys show higher compressive yield strength and ultimate compressive strength values.

The failure strain decreased with increasing amount of aluminium, with the Mg-10Al showing the highest value. The observed decrease in fracture strain with increased wt.% of Al is due to high content of secondary Mg<sub>17</sub>Al<sub>12</sub> phase, which results in plastic incompatibility with the surrounding α-Mg and aids as potential crack initiation sites<sup>8,11,14</sup>. This is particularly prominent in Mg-20 Al alloy wherein no yielding occurs, owing to the segregation of Mg<sub>17</sub>Al<sub>12</sub> phase<sup>7,8,10,11</sup>. The strengthening mechanisms that contribute towards the enhancement of yield and compressive strengths upon addition of aluminium is due to: (i) active load transfer between α-Mg and Mg<sub>17</sub>Al<sub>12</sub> phase<sup>8,10,15</sup>, (ii) increased content of high strength Mg<sub>17</sub>Al<sub>12</sub> phase<sup>8,10</sup>, (iii) grain refinement<sup>4,12,16</sup>, and (iv) increased density of dislocations owing to thermal stresses arising as a result of difference in linear coefficient of thermal expansion between α-magnesium and Mg<sub>17</sub>Al<sub>12</sub> phase<sup>17</sup>. From tensile stress-strain plot shown in Fig. 4, Mg-10Al samples show higher compressive ductility than Mg-15Al and Mg-20Al. Further, the absence of yield point in Mg-20Al alloy is evident.

**3.3.3 Fractography**

The macroscopic compressive fracture surfaces samples of the developed alloys showed shear fracture that occurred at approximately 45 to 50 degrees with respect to the compression test axis (Fig. 5 (a-c)). Macroscopic observation revealed that with the increase in addition of Al, the materials becomes more brittle as seen in the Mg-20Al alloy (Fig. 5 (c)), which has broken into multiple pieces.

Table 3 — Microhardness values of Mg-Al binary alloys (Al = 10, 15 and 20 wt. %).

Material	Microhardness (HV)	Increase in microhardness values when compared to AZ91 alloy
Mg-10Al	113.4 ± 0.9	88%
Mg-15Al	150.2 ± 1.6	150%
Mg-20Al	220.0 ± 1.0	265%
Pure Mg <sup>12</sup>	47 ± 2.8	-
Mg-9Al <sup>13</sup>	98 ± 1.8	-
AZ91 <sup>13</sup>	60	-

Table 4 — Compression properties of Mg-Al binary alloys (Al = 10, 15 and 20 wt. %). (% Increment in CYS and UCS with respect to pure Mg are mentioned in brackets)

Material	0.2 CYS (MPa)	UCS (MPa)	Fracture Strain (%)	Work of Fracture (MJ/m <sup>3</sup> )
Pure Mg <sup>12</sup>	74 ± 3	235 ± 8	22.7 ± 0.9	39.0 ± 2.3
Mg-10Al	232 ± 7 (215%)	545 ± 19 (130%)	19.0 ± 1.0	63.0 ± 5.8
Mg-15Al	346 ± 15 (365%)	458 ± 6 (95%)	8.4 ± 0.4	23.7 ± 0.9
Mg-20Al	-	484 ± 9 (105%)	5.3 ± 0.2	12.9 ± 0.1

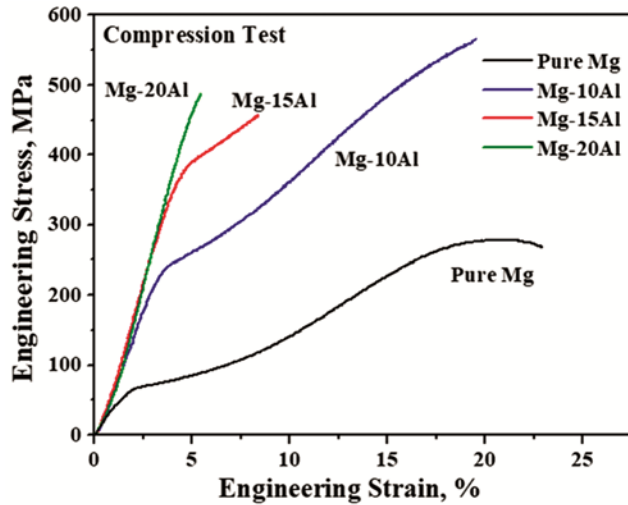


Fig. 4 — Compressive stress-strain plots of Mg-Al binary alloys (Al = 10, 15 and 20 wt. %).

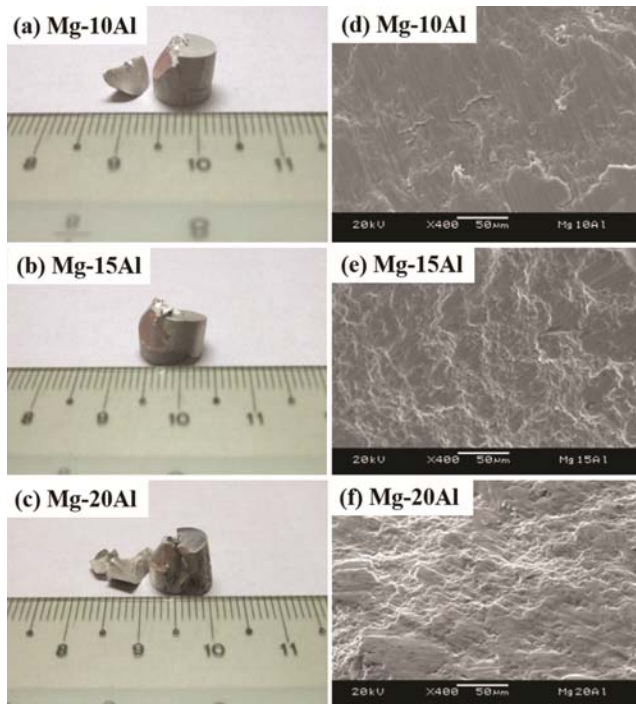


Fig. 5 — Macroscopic compressive fracture surfaces and SEM fractographs: (a,d) Mg-10Al, (b,e) Mg-15Al and (c,f) Mg-20Al alloys respectively.

Figure 5(d-f) shows the scanning electron microscopic images of the fractured surfaces. The fracture surfaces become rough with increase in aluminium content, which corroborate with the failure strain values. Surface roughness appears due to the hard  $Mg_{17}Al_{12}$  phase getting sheared along with the relatively soft  $\alpha$ -Mg matrix. Mg-10Al alloy had

relatively smoother surface due to the comparatively lower content of the  $Mg_{17}Al_{12}$  intermetallic phase. Amongst the developed alloys, the Mg-10Al alloy showed the best performance in terms of work of fracture, *i.e.* combination of strength and ductility, which is an indicator of material toughness.

#### 4 Conclusions

Mg-Al alloys with Al = 10, 15 and 20 wt. % (DMD + hot extruded) were examined for structural characteristics and mechanical behaviour. Increase in aluminium content increased the  $Mg_{17}Al_{12}$  formation. Morphology and content of  $Mg_{17}Al_{12}$  intermetallic phase was dependent on the Al-content, as was seen in the Mg-20Al alloy, in which the intermetallic phase segregated and clustered. The developed Mg-Al alloys showed remarkably high microhardness values owing to increased formation of inherently hard  $Mg_{17}Al_{12}$  intermetallic. The hardness values were higher than commercially used AZ91 alloy, such that Mg-20Al showed hardness increase by > 250%. The increasing amount of aluminium resulted in higher compressive yield strength and ultimate compressive strength values. The increase in strength values was influenced by Al-content and in turn on the content of  $Mg_{17}Al_{12}$  intermetallic phase. Mg-10Al alloy showed about 215% and 130% enhancement in yield and ultimate strengths respectively, with respect to pure Mg. This alloy showed the best properties in terms of work of fracture, which is representative of the alloy's toughness, *i.e.* strength + ductility combination. This work emphasizes the possibility of achieving improved mechanical properties of magnesium by incorporating unconventional amount of the major alloying element, namely aluminium.

#### References

- 1 Gaines L, Cuenca R, Stodolsky F & Wu S, *Potential Applications of Wrought Magnesium Alloys for Passenger Vehicles*, Report, Argonne National Laboratory (1995).
- 2 Avedesian, M M & Baker H, *ASM Specialty Handbook: Magnesium and Magnesium Alloys*, ASM International: Materials Park, Ohio, USA (1999).
- 3 Alderman M, Manuel M V, Hort N & Neelameggham N R, *Magnesium Technology*, The Minerals, Metals & Materials Society John Wiley & Sons, USA (2014).
- 4 Gupta M & Sharon N M L, *Magnesium Alloys and Magnesium Composites*, John Wiley & Sons, New Jersey (2011).
- 5 Emley E F, *Principles of Magnesium Technology*, Pergamon Press, London, UK, 1966.
- 6 Okamoto H, *J Phase Equilibria*, 19 (1998) 598.
- 7 Nguyen Q B, Fan Yi & Tun K S, *J Mater Sci*, 47 (2012) 234.

- 8 Jayalakshmi S, Kailas S V & Seshan S, *Composites-A*, 33 (2002) 135.
- 9 El-Amoush A S, *J Alloy Compds*, 463 (2008) 475.
- 10 Dargusch M, Dunlop G L & Pettersen K, Verksstoff-Informationen Gesellschaft, Wolfsburg, Germany (1998).
- 11 Jayalakshmi S, Arvind S R & Chen X Z, *JOM*, 4 (2020) 1.
- 12 Jayalakshmi S, Sankaranarayanan S, Koh S P X & Gupta M, *J Alloys Compds*, 565 (2013) 56.
- 13 Jayalakshmi S, Dezhi Q, Sankaranarayanan S & Gupta M, *Int J Microstructure Mater Prop*, 8 (2013) 283.
- 14 Nguyen Q B & Gupta M, *Mater Sci Eng A*, 527 (2010) 1411.
- 15 Nguyen Q B & Gupta M, *J Composite Mater*, 43 (2009) 5.
- 16 Dieter G E, *Mechanical Metallurgy*, McGraw-Hill, SI Metric Edn, USA (1988).
- 17 Dini H, Andersson N E, Ghassemali E & Jarfors A E, *Magnesium Technology*, Edited by: Manuel M V, Singh A, Alderman M & Neelameggham N R, TMS-The Minerals, *Metal Mater Soc*, USA (2015).